IEEE Access
Multidisciplinary | Rapid Review | Open Access Journal

Received 6 November 2022, accepted 20 December 2022, date of publication 13 January 2023, date of current version 9 February 2023.

Digital Object Identifier 10.1109/ACCESS.2023.3236812

RESEARCH ARTICLE

Detecting COVID-19 From Lung Computed Tomography Images: A Swarm Optimized Artificial Neural Network Approach

S. PUNITHA[1], THOMPSON STEPHAN[2], (Member, IEEE), RAMANI KANNAN[3], (Senior Member, IEEE), MUFTI MAHMUD[4,5,6], (Senior Member, IEEE), M. SHAMIM KAISER[7], (Senior Member, IEEE), AND SAMIR BRAHIM BELHAOUARI[8]

[1]Department of Computer Science and Engineering, Graphic Era (Deemed to be University), Dehradun, Tamil Nadu 248002, India
[2]Department of Computer Science and Engineering, Faculty of Engineering and Technology, M. S. Ramaiah University of Applied Sciences, Bengaluru, Karnataka 560054, India
[3]Department of Electrical and Electronics Engineering, Universiti Teknologi PETRONAS, Seri Iskandar 32610, Malaysia
[4]Department of Computer Science, Nottingham Trent University, NG11 8NS Nottingham, U.K.
[5]Medical Technologies Innovation Facility, Nottingham Trent University, NG11 8NS Nottingham, U.K.
[6]Computing and Informatics Research Centre, Nottingham Trent University, NG11 8NS Nottingham, U.K.
[7]Institute of Information Technology, Jahangirnagar University, Savar, Dhaka 1342, Bangladesh
[8]Division of Information and Computing Technology, College of Science and Engineering, Hamad Bin Khalifa University, Education City, Qatar Foundation, Doha, Qatar

Corresponding author: Samir Brahim Belhaouari (sbelhaouari@hbku.edu.qa)

ABSTRACT COVID-19 has affected many people across the globe. Though vaccines are available now, early detection of the disease plays a vital role in the better management of COVID-19 patients. An Artificial Neural Network (ANN) powered Computer Aided Diagnosis (CAD) system can automate the detection pipeline accounting for accurate diagnosis, overcoming the limitations of manual methods. This work proposes a CAD system for COVID-19 that detects and classifies abnormalities in lung CT images using Artificial Bee Colony (ABC) optimised ANN (ABCNN). The proposed ABCNN approach works by segmenting the suspicious regions from the CT images of non-COVID and COVID patients using an ABC optimised region growing process and extracting the texture and intensity features from those suspicious regions. Further, an optimised ANN model whose input features, initial weights and hidden nodes are optimised using ABC optimisation classifies those abnormal regions into COVID and non-COVID classes. The proposed ABCNN approach is evaluated using the lung CT images collected from the public datasets. In comparison to other available techniques, the proposed ABCNN approach achieved a high classification accuracy of 92.37% when evaluated using a set of 470 lung CT images.

INDEX TERMS Artificial neural networks, artificial bee colony algorithm, multilayer perceptron, resilient backpropagation, texture features, feature extraction, classification accuracy.

I. INTRODUCTION

The Novel Coronavirus disease named COVID-19 is a dangerous one that leads to death causing severe pneumonia in the lung regions. This novel virus started in 2019 and has spread affecting almost all the countries around the globe recording 427,192,984 cases till 22/02/2022 [1]. A complete cure has not been discovered and hence early and accurate diagnosis can only be the remedy of COVID-19 that can decrease the mortality rate [2]. COVID-19 contains a positive single-stranded RNA type and, hence, it is difficult for medical professionals to discover preventive medicine for its mutating nature. Countries such as the United States, the United Kingdom, China, Italy, Spain, Iran, and others have a high death rate, particularly among the elderly. COVID-19 has been seen in bats, pigs, dogs, humans, poultry, and cats. Common symptoms include throat pain, fever with headache, cough, runny nose, and it mostly affects people with a weak

The associate editor coordinating the review of this manuscript and approving it for publication was Rajeswari Sundararajan.

immune system [3], [4]. This spreading mode of this virus is air transmission and spreads among humans through hand contact, mucus contact, or breath contact [5], [6].

Artificial intelligence (AI) and machine learning (ML) have been widely used in diverse research areas, including anomaly detection, disease diagnosis, text mining, cyber security, etc. [7], [8], [9], [10], [11], [12], [13], [14], [15], [16], [17], [18], [19], [20], [21], [22], [23], [24], [25], [26], [27], [28], [29], [30], [31], [32], [33], [34], [35], [36], [37], [38], [39], [40]. Artificial Neural Networks (ANN) has been used in image segmentation and classification [41], [42]. Coronavirus causes severe pneumonia that can be diagnosed using chest X-ray or lung CT scan images [43]. Many types of research that diagnosed various deadly diseases have successfully used Multi-Layer Perceptron (MLP) as the prediction method [44], [45]. Appropriate selection of the parameters of the MLP network can increase the accuracy rate of the diagnosis. Swarm intelligence algorithms have been widely used in the literature to fine-tune the input parameters and also the other design parameters of an ANN model. The input features, hidden node size, hidden layer size, learning rate, momentum constant, and the initial weights are the various parameters considered for optimal ANN design.

Sun et al. [46], proposed an adaptive feature selection method for choosing contrasting features for the analysis of COVID-19. It majorly concentrates on high-level feature selection. It is the process of extracting location-specific features such as where it has spread and how much it has spread. After that, affected regions are segmented. They have considered various features that use interlobular septal deepening for classification. Computer Aided Diagnosing method determines only the bilateral lobe. In this approach, lung lobes, bilateral lungs, and pulmonary segments are considered for better segregation. It also calculates the distribution. To reduce the redundancy of the features, Xgboost and the random forest method are used. The dataset includes 1495 COVID-19 and 1027 pneumonia patient details. It achieves 91.79% accuracy. Carvalho et al. [47] designed the system for the diagnosis of COVID-19. CT-images are taken as input. For classification, CNN and XGBoost are used. This approach involves i) generation of CT photographs ii) eradication of feature which uses CNN iii) class of images which makes use of XGBoost and iv) affirmation of outcomes which includes metrics typically utilised in CAD systems. The technique proposed used CNN for the utilisation of features in CT images and XGBoost for grouping. 708 CT images are collected. In that data set, 312-COVID-19 and 396 non-COVID. It focuses mostly on the binary class. In general, to train the deep convolution neural network architecture, we need massive volume of CT images. As 708 CT-images are not sufficient to train CNN, they used pretrained models for feature extraction and eXtreme Gradient Boosting (XGBoost) for classification. This technique produced 95.07% accuracy. Wang et al. [48], proposed an automated system for extracting pneumonia lesions from CT images. Splitting of images is very essential for correct prediction, which requires follow-ups. Specifically, deep learning helps in performing this kind of image splitting. But, it requires a large volume of high quality annotations. If the quantity of the data set is minimal, then training the CNN seems to be backbreaking. Hence, a novel noise-robust framework was proposed which learns from the noisy labels for segmentation tasks. It presents the discrepancy between foreground and background pixels and labels, which are noisy in general. In which, the advanced COVID-19 Pneumonia lesion segmentation network (COPLE-Net) is used to increase information gain. It combines the uses of max polling and average pooling as well as down sampling. It minimises information loss compared to simple max pooling. For experimentation, it utilises the CT images of 558 Corona patients. Wang et al. [49] presented an enfeebled supervised system for coronavirus segregation and localization of lesions from chest CT. It really works on the extraction of images part. For every patient, the lung vicinity became segmented by utilising a pretained UNet; then the 3-D lung vicinity became segmented and fed right into a 3-D deep neural technique to find out the chance of occurrence of the coronavirus. 499 CT scan images have been utilised for training. For testing, 131 CT volumes have been used. 1.93 seconds are taken by the system to determine each patient's CT volume, which uses a dedicated graphics processing unit. Authors have adapted the 3-D deep convolution neural community to identify COVID-19 from CT volumes. It directs CT extent and 3-D lung as input. The 3-D lung masks are generated through pretrained U-Net. DeCoVNet consists of three phases, namely: network stem to preserve rich local visual information; the next phase is a 3D residual block to extract the features; the last phase is a progressive classifier, which classifies whether the person is affected by COVID-19 or not. El-Sayed et al. [50] proposed inventive feature selection and voting classifier algorithms, especially for the coronavirus. Diagnosis plays a vital role in providing timely and suitable treatment. In this approach, numerous deep learning algorithms (PSO, CNN, and Guided Whale Optimisation algorithm) are experimented with. A novel voting approach is implemented to overcome individual classifier incompatibilities. Sakib et al. [51] proposed a deep learning-based chest radiograph type system for accurately distinguishing COVID-19 cases. A novel data set is prepared, including normal, pneumonia, and COVID-19 cases. The Posteroanterior (PA) chest view is chosen as a feature for classification which improves the quantity of the data set. A data augmentation for radiographic images algorithm is used to generate the augmented data. For the classification of COVID-19, Rajaraman et al. [52] employed excellent deep learning ensemble techniques. It uses chest X-rays as a data set. The data set combines X-ray images of bacterial pneumonia, COVID, and viral infection.Numerous pruning models are combined through ensemble techniques. It results in better classification with

an accuracy of 99.01%. For recognising COVID-19 from CT-images, Mishra et al. [53] employed deep convolution neural network architecture. A decision fusion-based strategy is applied in this case. To get at the final prediction, it checks a number of deep learning models. The goal of this model is to diminish the bias of individual approaches via major voting approaches. They experimented with different models like VGG 16, Inception V3, ResNet50, Dense Net 121, and Dense Net201. Specificity, accuracy, sensitivity, precision, recall, and F1-Score are taken as performance metrics. Singh et al. [54] Multi-objective differential evolution based convolution neural networks are implemented to classify the patients affected by COVID-19. CT images are taken as a data set. It focused only on binary classification. A multi-objective differential evolution based convolution neural network is used for classification. In this approach, stride, kernel size, activation functions, kernel type, padding, hidden layer, etc. are considered as parameters to train the machine. Numerous deep convolution neural network architectures such as CNN, ANN, and ANFIS are being experimented with to get accurate classification. Goel et al. [55] have proposed deep network architectures for finding the infections caused by COVID-19 using CT images. The random forest algorithm uses the features derived from the auto encoder and grey level co-occurrence matrix for efficient and fast detection of COVID-19. The data set includes 2482 CT images,among which 1252 images are those of the victims tested positive for the COVID-19 infection and 1230 images are from individuals tested negative for the coronavirus. Auto encoders are used to recreate the given image. Encoders are used for dimensionality reduction. It also tries to reduce overfitting. GLCM is utilised for texture evaluation due to the fact that it is able to estimate the quality of the image with respect to second order statistics. The pixel relationships are studied by using a grey level co-occurrence matrix. Jain et al. [56] presented a model for COVID-19 exposure and analysis on chest X-ray images. Post Anterior (PA) vision of chest X-ray images is considered to classify the diseases. For comparative analysis, Inception V3, Xception, and ResNet models are furnished for comparison. The data set includes 6432 chest x-ray samples, of which 5467 were applied for preparation and 965 images were used for validation. In this study, the Xception model earned better accuracy (97.97%) than other models. A few recent applications of optimization algorithms are given in [83], [84], [85], and [86]. The contributions of the paper are as follows:

- This paper introduces a CAD system called the ABCNN approach for the detection and classification of the COVID-19 disease.
- This paper uses a publicly available dataset that contains lung CT scan images of COVID-19 cases (COVID pneumonia) and non-COVID-19 (normal pneumonia or other infections).
- The proposed system uses a swarm intelligent optimisation variant inspired by the foraging behaviour of honey bees called the Artificial Bee Colony (ABC) optimisation technique for the generation of the optimal threshold for a region-growing segmentation process, input features, hidden nodes, and the initial weights for a feed-forward neural network that is trained and tested over a set of COVID-19 and non-COVID-19 cases.
- The proposed system first preprocesses the lung CT images using a Wiener filter and then segments the lung regions.
- Further, rectangular patches of the areas of Regions of Interest (ROI) are cropped from the infected regions.
- Then a region-growing segmentation process whose thresholds are optimised using an ABC optimisation process is used for accurately segmenting the infected portions from the rectangular patches.
- Texture and histogram-based intensity features are extracted from the infected regions and an appropriate set of features is selected, which acts as the input feature set for the classification process.
- Further, the ABCNN approach uses a fine-tuned ANN model for the classification of the COVID-19 and non-COVID-19 cases.

This paper is summarised as follows: A review of some related works that have used various machine learning models is described in section II. Section III handles the detailed description of the proposed ABCNN approach. Section IV has the experimental analysis and assessment section followed by the conclusion in section V.

II. STATE-OF-THE-ART

An automatic diagnosis system for COVID-19 disease is proposed [57]. The CT lung images were collected from three different hospitals. These images contain infection regions of COVID-19, viral pneumonia, and other normal regions. The infectious regions are extracted using a 3D deep learning model. The type of infection and the confidence score are evaluated using the bayesian function. The proposed system attained an accuracy of 86.7% when tested on a set of 618 CT lung samples.

A diagnosis system for the feature extraction and classification of COVID-19, pneumonia, and normal lung CT images of 316 patients is proposed [58]. The CT lung images are preprocessed for the noise removal process. Histogram based thresholding is done for the extraction of lung portions. Each lung portion undergoes a feature extraction process where a set of deep learning features and entropy features are extracted. Further, a long short-term memory (LSTM) neural network is used to classify the lung portions as COVID-19, pneumonia, and normally based by taking the input features as input.

A neural system called COVNet, which is an automatic detection system for the detection of COVID-19, is proposed [59]. This system is evaluated using a dataset collected from 6 different hospitals that contains 4356 CT images of the chest belonging to 3,322 patients. The sensitivity and specificity for COVID-19 detections are 90% and 96% respectively. The proposed system uses a supervised

convolution neural network that uses ResNet50. This system takes CT image slices as input where CNN features are extracted from each of the slices and integrated using a max-polling operation. These features are fed to the connected layer to calculate a probability score.

A model for automatic COVID-19 diagnosis with the help of chest X-ray images is proposed [60]. This proposed system is used for binary and multiple class classification. The accuracy rate is 98.08% for COVID-19 and normal binary classification, where the accuracy rate is 87.02% for the classification of COVID-19, normal, and pneumonia multi-class classification. The proposed system used 17 convolution layers with filtering in each layer. This system is publicly available on GitHub for the initial screening and is available to radiologists.

A model based on deep learning is introduced for the diagnosis of COVID-19, which was evaluated on a dataset containing 1,119 CT pathogen images that contain cases of COVID-19 and viral pneumonia [61]. The region of interest is first extracted and then randomly selected. A convolutional neural network is used to extract the graphical features and a fully connected neural network is used for classification purposes. The testing accuracy reached 79.3% with a sensitivity of 0.67 and a specificity of 0.83.

A Convolutional Neural Network based model for the diagnosis of COVID-19 called DeCoVNet is proposed [62]. The proposed system works in different stages involving 2D-UNet preprocessing, DeCoVNet preprocessing, and Data Augmentation. The lung region is extracted with the help of Unet and then a 3D deep neural network is utilised to predict COVID-19 infectious. The proposed system obtained a ROC of 0.959 AUC. The sensitivity of the proposed system is 90.7% and its specificity is 91.1%.

A deep learning model is proposed for coronavirus diagnosis using chest X-rays [63]. The system uses a fuzzy color technique for the preprocessing and the dataset with the stacked images is used for training the deep learning networks called SqueezeNet and MobileNetV2, where the significant features are selected using social mimic optimisation. The SVM is used as the classifier that classifies the images as pneumonia, normal, and coronavirus affected. The classification rate achieved is 99.27%.

A machine learning method for the detection of COVID-19 is proposed using lung CT images is proposed [64]. A total of four patches of different sizes were extracted from the image, and a feature extraction process was done by deriving the texture features. An SVM classifier is used for the classification of the patches as COVID-19 pneumonia and other viral pneumonia using 2, 5 and 10-fold cross-validations. The classification accuracy attained is 99.68%.

A deep learning method called DeepPneumonia was developed for the diagnosis of COVID-19 [65]. The proposed system is evaluated using the CT images collected from 88 patients with COVID-19, 101 patients with bacterial pneumonia, and 86 healthy people. The regions of the lungs were extracted and the blacks were filled. The Details Relation Extraction neural network (DRE-Net) is further used to extract the K details of the CT images to obtain image predictions. Then, using the image predictions, the patient level diagnosis is achieved. The proposed system achieved a 0.95 AUC and 0.96 sensitivity.

A deep neural learning system is proposed for the automatic segmentation of the infected regions of COVID-19 [66]. The system is evaluated using a publicly available dataset of lung CT images. The proposed system is developed using the U-Net architecture. An aggregated residual transformation is used to increase the efficiency of U-Net. The proposed system with augmentation showed an accuracy of 79% and without augmentation of 70% when evaluated using 110 CT slices of 60 patients.

III. DETAILED DESCRIPTION OF PROPOSED ABCNN APPROACH

The proposed ABCNN system is composed of major steps such as image preprocessing to enhance the image quality, ROI extraction for finding out the infected portions, feature extraction for deriving the texture and intensity features, feature selection that selects the significant features, and classification to diagnose. The implementation of the ABCNN approach follows a simple and purely wrapper-based approach without the involvement of any statistical screening such as F-score, information gain, etc., on the dataset used. The work proposed in this paper using ABC optimisation for simultaneously optimising the segmentation, feature selection, and classification processes is novel. Figure2 shows the block diagram of the proposed fully automated ABCNN diagnosis system.

The input dataset is the lung CT scan image dataset. The total set is subdivided into three subsets. The first set obtains the 50% samples that can be used for training. The next 25% samples are utilised for validation and the rest of 25% is utilised for testing. The proposed approach derives the optimal set of input features using the ABC optimisation technique. Then optimal features are collected from the three subsets, eliminating the rest of the features. The optimal features from the training set are utilised for ANN classifier training. The optimal solutions (initial weights and hidden node size) generated by ABC are used as the initial parameter settings of ANN. The ANN error is calculated with the help of the validation set. The training of ANN is stopped if the validation error increases for six iterations continuously. The fitness of trained ANN is calculated using Equation (7 & 8). The ANN with high fitness (best) is selected and tested using the testing set with optimal feature subsets.

Solution representation is given in Figure1. A bit gives the random initial weights, in which 2^A different initial weights can be explored. B bits give the hidden node size so that 2^B hidden node size can be explored. C bits give the feature bits that represent the total features. If a feature is selected, then the 'C' bit is one; otherwise, it's zero. D bits represent the threshold values where 2^D threshold values can be explored.

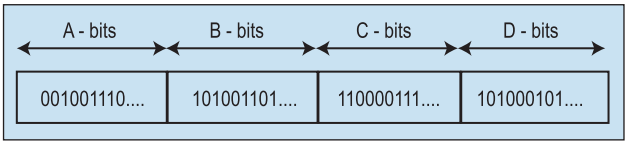

FIGURE 1. Initial solution representation.

A. IMAGE ACQUISITION

The proposed ABCNN approach uses the lung CT scan images, which are abnormal. These images acquired contain infectious regions of COVID-19 pneumonia and COVID-19 (normal, bacterial pneumonia, and other infections). A set of 470 CT lung images were acquired from [67] which is a publicly available data set that contains CT lung images collected from patients suspected of various lung infections. The proposed work uses 275 lung CT scan images of COVID-19 and 195 lung CT images of non-COVID-19 from [67]. These images are used by the ABCNN approach for training, validation, and testing for segmentation and classification purposes. The sample images from the data set with the radiologist's markings in arrows and circles that show the infected regions are shown in Figure 3.

B. PRE-PROCESSING

The preprocessing step removes unwanted noise, which enhances the image quality. The Wiener filter is used to remove noise where the edges and the fine details of the lungs are preserved. These filters are used for the over-smoothing of the image. Original and Wiener filtered images are shown in Figure 4. Wiener filtering calculates the local mean and variance of the local neighbourhood of every pixel. Further, pixel-wise linear filtering is done using Equation 1.

$$Z(x, y) = m + \frac{(v^2 - n^2)}{v^2} * (J(x, y) - m) \tag{1}$$

Z represents the filtered image; J represents the original image; m and v represent the mean and variance of the local neighborhood, respectively, and n represents variance related to noise.

C. EXTRACTION OF REGION OF INTEREST (ROI)

The region of interest in extraction consists of two stages. The first stage involves the extraction of the lung region from the lung CT image acquired, where the second stage involves the extraction of the infected regions from the lung portions. The ABCNN approach incorporates the extraction of ROI only on the abnormal images. The entire set of images is fed as the input to an ANN classifier with the texture features of those images as the input. The ANN then classifies those images as normal and abnormal. Further, the abnormal images are considered for the ROI extraction process where histogram-based thresholding is used for the extraction of lungs and the optimal thresholds are generated for a region-growing process for the segmentation of the infected regions.

1) EXTRACTION OF LUNG REGIONS

Preprocessing extracts the useful regions (lung regions) without losing their quality. The lung regions of a CT lung scan image are superimposed on its background. The ROI (lung region) consists of the infected and background region information. This extraction stage separates the lung regions from their background using a global thresholding technique in the lung CT. Let us take a lung CT image $Z(x, y)$, which consists of two lung regions with the infected portions around a dark background. The lung region can be extracted from its background using a threshold T represented using Equation 2.

$$Z(x, y) = \begin{cases} j & \text{if } j(x, y) > T \\ 0 & \text{if } j(x, y) \leq T \end{cases} \tag{2}$$

Any point (x, y) on the image for which $J(x, y) > T$ is considered as the lung region. The other pixel points are considered background regions. The appropriate thresholds are chosen from the histogram of the lung CT image. A histogram-based on intensity is constructed for the image, and a local threshold is selected by analysing the intensity levels of the local region around a pixel. The lungs are segmented and further processing is done on the lung regions. Figure 5 shows the binary and grey lung regions obtained.

2) EXTRACTION OF THE INFECTED REGION

The segmentation of the infected region separates the infected portions from the lung region of the COVID-19 CT scan image. Two commonly used segmentation methods for non-trivial images are region-based segmentation methods based on similarity detection, such as region growing, and boundary-based segmentation methods based on discontinuity detection, such as thresholding and gradient edge detection, in which discontinuities are detected and linked to form region boundaries. The proposed ABCNN approach uses an optimised region growing method for segmenting the infected portions of the lung region. Figure 6 shows the infected region after extraction. The procedure for the proposed ABC optimised region growing process is as follows.

Step 1. Input the abnormal segmented lung section of the CT image.
Step 2. Generate the optimised threshold by ABC algorithm represented by α.
Step 3. Let α be considered as the seed point for the proposed region growing process.
Step 4. Add the four neighborhood pixels.
Step 5. Evaluate distance (β) between new neighbor pixels mean intensity and region mean intensity.
Step 6. Perform region growing process if $\alpha \leq \beta$ and include the neighbor pixel nearest to the region mean intensity if the new pixel is not included already and save new pixel coordinates.
Step 7. Save the new region mean and return to **Step 2**.

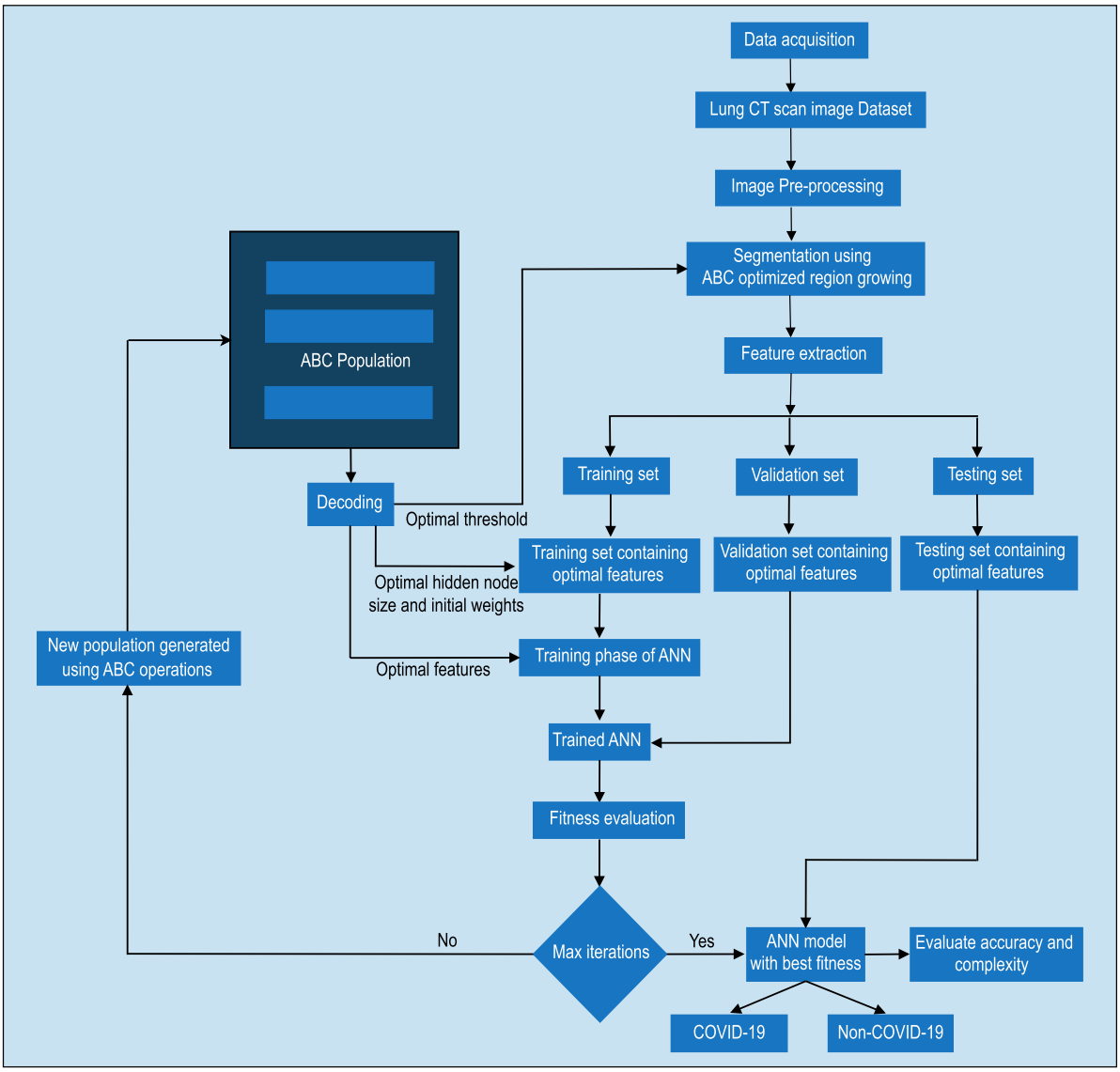

FIGURE 2. The proposed architecture of ABCNN approach.

FIGURE 3. Samples of lung CT scan images.

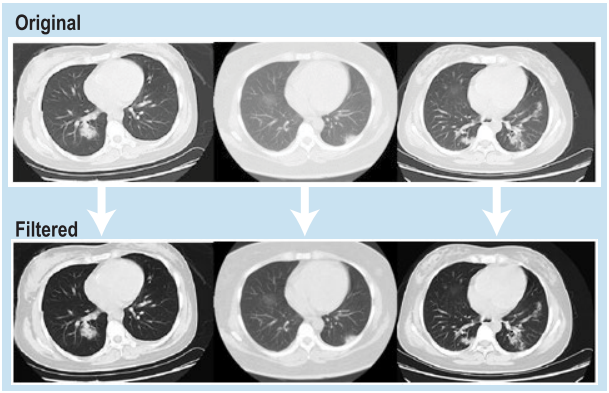

FIGURE 4. Original and wiener filtered images of lung CT images.

Step 8. Perform region growing till every similar pixel is grouped.

Considering the fact that the infected parts in the lung region do not share the same intensity levels, choosing a constant threshold to segment the infected parts using region-wide growth leads to inaccuracy in the segmentation of the infected parts. As a result, an automated method is necessary for the estimation of an appropriate threshold. To end this, a metaheuristic swarm intelligence-based technique inspired using the foraging of honey bees called Artificial Bee Colony introduced in 2005 by karaboga and used for

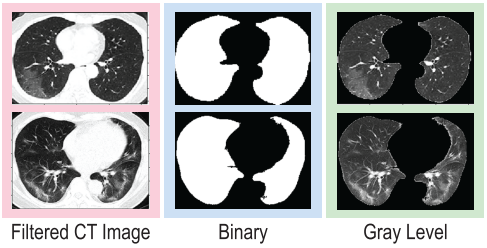

FIGURE 5. Lung extraction from filtered CT images. The filtered CT lung image is seen in the left, the binary lung extraction from the filtered CT lung image is in the middle and the gray level lung extraction of the filtered CT lung image is on the right.

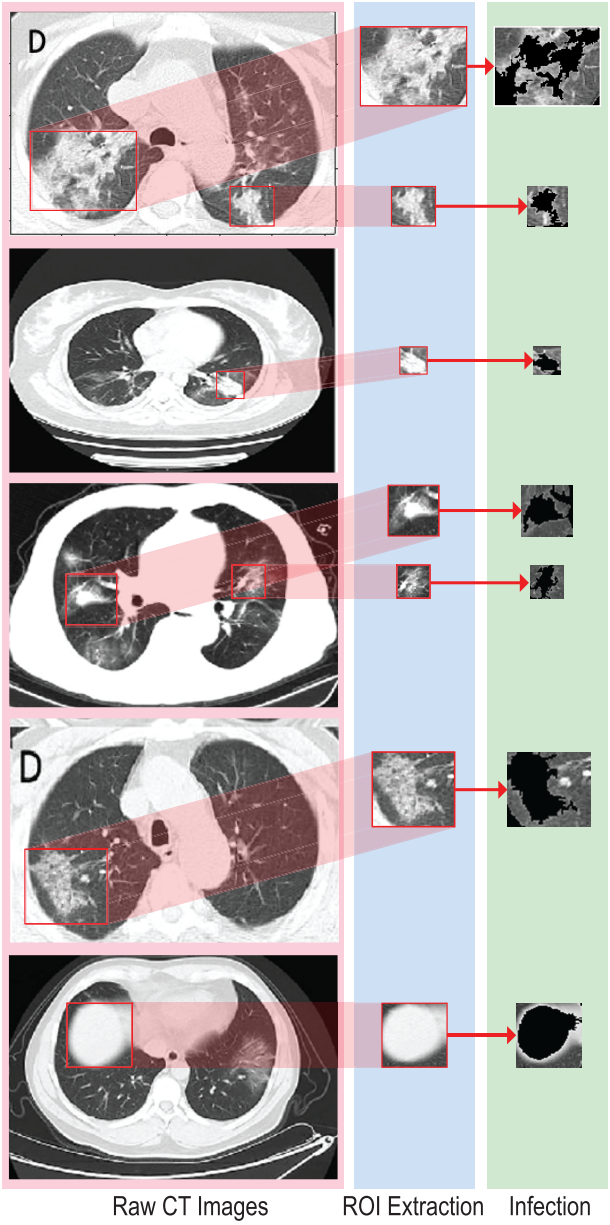

FIGURE 6. Infected region detection from raw CT lung image through region of interest extraction.

various applications as demonstrated in [68] and [69] is utilised for the generation of a dynamic threshold instead of using a static threshold throughout the segmentation process. ABC is a stochastic search process and has been proved to solve multidimensional problems and real-time optimisation problems. It is robust and simple, with a minimum number of control parameters. The algorithmic steps for the generation of the optimal threshold using ABC optimisation that can be used in the segmentation of the infected regions are described as follows.

Step 1: Initialization (Generate possible thresholds): Each food source represents a possible threshold that is randomly produced in the range [-10, 10] using Equation 3.

$$E_k^l = E_k^l + random(0,1) * (E_{max}^l - E_{min}^l) \quad (3)$$

E_k^l is the k^{th} food source with parameter l and $k = 1, 2, \ldots, S$, where S represents maximum food sources. $l = 1, 2, \ldots, d$, where 'd' gives the dimension indicating the number of parameters of the optimisation problem. E_{min}^l and E_{max}^l gives the minimum and maximum bound of l^{th} parameter of the optimisation problem respectively.

Step 2: Quality Evaluation of food source (Evaluate segmentation process): The fitness values for each food source E_k are identified using Equation4.

$$fitness = X \times Y(\sum_{i=1}^{X}\sum_{j=1}^{Y} M_{ij} \oplus T_{ij}) \quad (4)$$

here $X \times Y$ represents the size of the image, (i, j) gives the location of the pixel of the manually segmented binary image and the binary image segmented using the proposed ABC optimised region growing. Equation 4 gives the unequal pixels in the manual and segmented images by the proposed approach. Subtracting the produced value of Equation 4 from the total size of the image $X \times Y$, the equal pixels in compared images can be obtained.

Step 3: Employed bee Phase (Search for a better local optimal threshold): Food sources representing the possible solution (threshold) are assigned to employee bees. Employee bees use Equation 5 and search for neighborhood food sources around the current food sources E_k^l.

$$V_k^l = E_k^l + random(-1,1) * (E_k^l - E_v^l) \quad (5)$$

here, E_d represents a random food source where $v \in 1, 2 \ldots, S$. 'k' is a random integer and $l = 1, 2 \ldots, d$ and 'v' is not equal to 'k' for proper exploitation. If the quality of V_k^l is higher than E_k^l then bee eliminates E_k^l saving V_k^l, or vice versa.

Step 4: Onlooker Bee Phase (Generating a local optimal threshold): Information regarding the selected food sources is shared with the onlooker bees. The probability value Z_i of each food source

TABLE 1. Texture and intensity features extracted.

Feature Labels	Feature Name
Intensity Histogram features (f1, f2, f3, f4, f5)	Entropy Skewness Mean Variance kurtosis
Texture features (f6, f7, f8, f9, f10, f11, f12, f13, f14, f15, f16, f17, f18, f19, f20)	Information measure of correlation Long Runs Emphasis Short Runs Emphasis Energy Cluster Prominence Contrast Dissimilarity Run Length Non-Uniformity Run Percentage Homogeneity Maximum probability Gray Level Non-Uniformity Sum of squares Entropy correlation Contrast

received from the employee bee is calculated using Equation 6.

$$Z_k = \frac{fitness(A_k)}{\sum_{k=1}^{N} fitness(A_k)} \tag{6}$$

The quality of the food source A_k is represented as $fitness(A_k)$. The value Z_k of food source is compared with a random (0,1). Food sources with a Z_i value greater than random (0,1) are selected by the onlooker bees.

Step 5: Food source memorization (Save the optimal threshold generated): Food source with high $fitness(E_k)$ is memorized.

Step 6: Scout Bee Phase (Generating new thresholds for the next iteration in search of a global optimal threshold): In this phase, food sources that are not improved for certain iterations are identified and replaced by a randomly generated food source using Equation 3.

3) FEATURE EXTRACTION

In this proposed work, features indicating the intensity histogram and texture features are extracted from the segmented infectious regions to indicate the characteristics of segmented infectious regions. In comparison to the rest of the regions in CT images, infected portions appear with high intensity levels. The COVID-19 infected portions of the lungs have an erratic texture compared to other infectious regions of the lungs. Hence, textural features are extracted using a gray-level co-occurrence matrix (GLCM) and gray-level run-length matrix (GLRLM) that contains the second-order statistical information regarding the neighbouring pixels of the image. The extracted features are given in Table 1.

D. FEATURE SELECTION AND CLASSIFICATION

The proposed ABCNN approach performs optimal feature set selection and ANN design parameter selection, such as initial weights and hidden node size. Feature selection selects appropriate features from features that are extracted. It improves classification accuracy, decreasing the computational cost [70]. Feature selection is an optimisation problem that searches for solutions in a large set of solution spaces (different features). Appropriate initial weights and hidden node size may prevent the ANN from being overtrained or undertrained and improve the convergence of the training process. Due to the importance of simultaneous optimisation of ANN design parameters and feature selection process and because of the complex design issues of ANN, ANN topology optimisation can be hybridised with a powerful swarm metaheuristic optimisation, such as ABC, because of its powerful local and global search capabilities in finding out global optimal solutions. The steps for implementation of the proposed work are explained as follows.

Step 1: Initialization (Generating the possible feature set, initial weights, and hidden node size):
Each Food source represents a possible set of features, initial weights, and hidden node size that are randomly produced using Equation1.

Step 2: Decoding process: Decode each solution obtained for selecting the optimal feature subset, initial weights, and hidden node size. Only the selected features are utilised and the remaining are eliminated from training, validation, and testing dataset.

Step 3: Training process: Using the MLP design parameters obtained from step 2, such as input features, initial weights, and hidden node size, the training process is executed using the training set. The problems of over-training MLP are avoided by monitoring the validation set error while the training process is executed. The training is stopped if the NN error on the validation set increases for six iterations continuously.

Step 4: Quality Evaluation of food source (Evaluating the ANN): The fitness values for each food source E_k identified using $NNerror = (Q_{max} - Q_{min}/s * t) \sum_{i=1}^{s} \sum_{j=1}^{t} (X_j^i - Y_j^i)$. ANN fitness is calculated using Equation 8. A higher NN error represents low fitness ANN.

$$NNerror = (Q_{max} - Q_{min}/s * t) \sum_{i=1}^{s} \sum_{j=1}^{t} (X_j^i - Y_j^i) \tag{7}$$

$$Fitness = (1/NNerror) \tag{8}$$

's' and 't' represents the size of output nodes and validation sample size, respectively. Q_{max} and Q_{min} give the maximum and minimum output (actual),respectively. Y_i^j and X_i^jgive the maximum and minimum output (actual),respectively.

Step 5: Employed bee Phase (Searching for a better local optimal input features, initial weights, and hidden node size): Food sources representing the possible solution (initial weights, hidden node size, and input features) are assigned to employee bees. Employee bees use Equation3 and search for neighborhood food sources V_k^l around the current food sources E_k^l.They perform a greedy selection between V_k^l and E_k^l to select the better one.

Step 6: Onlooker Bee Phase (Generating local optimal input features, initial weights, and hidden node size): The food sources that are selected by the employee bees is evaluated using Equation 6. Then, a better food source (initial weights, hidden node size, and input features) that are selected are again exploited using the Equation 5.

Step 7: Food source memorization (Save the optimal input features, initial weights, and hidden node size generated): Food source with high $fitness(A_k)$ using Equation 8 is memorized.

Step 8: Scout Bee Phase (Generating new input features, initial weights, and hidden node size for the next iteration in search of a globally optimal solution): In this phase, food sources that are not improved for certain iterations are identified and replaced by a randomly generated food source using Equation 3.

Step 9: Final network and performance calculation: Iterations are evaluated until the final generation is attained. The solutions with the best fitness will be selected in the final generation. Using the test data set, the ANN accuracy and complexity are evaluated. The proposed approach calculates the ANN complexity (number of connections) using the following equation.

$$Con = O * P + P * Q + P + Q \tag{9}$$

where 'O' gives input features (size), 'P' indicates hidden node size, and 'Q' indicates output nodes (size). The MLP with fewer connections guarantees the least complexity.

IV. PERFORMANCE EVALUATION OF THE PROPOSED ABCNN APPROACH

To evaluate the performance of the proposed ABCNN approach on COVID-19 diagnosis, a total of 470 CT scan images, of which 275 CT COVID-19 images and 195 non-COVID images collected from [67] were used for training, testing, and validation purposes. The images undergo the texture feature extraction process and are fed into an ANN classifier where they are classified as normal and abnormal. Then, after the extraction of lung regions from the abnormal images, patches containing the infected regions are cropped and fed as the input to the ABCNN approach. The results acquired are presented as segmentation and classification performance for the proposed ABCNN approach.

TABLE 2. Parameter settings of ANN.

Parameter	Value
Training	Backpropagation
Input nodes size	20
Output nodes size	2
Initial weights (Number of bits)	15
Hidden node size (Number of bits)	2
Input features (Number of bits)	20
Activation function (hidden node)	Hyperbolic Tangent
Activation function (output node)	Pure Linear
Training set (no of samples)	235 (50%)
Validation set (no of samples)	117 (25%)
Testing set (no of samples)	118 (25%)

TABLE 3. Parameter settings of ABC.

Parameter	Value
Employee Bees (size)	30
Onlooker Bees (size)	30
Scout bees (size)	1
Total colony (size)	60
Number of iterations	30
Number of runs	10
Count limit	10

TABLE 4. Segmentation results of the ABCNN approach as seen in Figure 7.

Images	DICE (%)	Jaccard (%)
1	0.91	0.88
2	0.90	0.87

A. PARAMETER SETTINGS AND EXPERIMENTAL SETUP

The proposed methodology is implemented using MATLAB (software MATLAB version R2019a) on a PC with the following characteristics: The Intel Pentium i5 8th generation processor, 8 GB of RAM, and the Windows-10 operating system. The neural network toolbox is used for backpropagation training. The training parameters for the implementation of backpropagation are the default. The winner-takes-all approach is used for classification at output nodes. The parameter settings of the ANN are shown in Table 2. The number of input nodes is set equal to the input feature size, which is 20, and the number of output nodes is set to two, representing the COVID-19 and COVID-19 classifications. The initial weights (A) in terms of number of bits is set as 15 where 2^A different combinations of initial weights can be explored. The hidden node size (B) is set as two, which indicates that it indicates 2^B different combinations of hidden node sizes can be explored. The input feature size (C) in terms of the number of bits is set at 20, where the value '1' indicates the feature is turned on or '0' indicates the feature is turned off. Fifty percent of the total dataset is taken for training purposes. That comes to 235 images. The remaining fifty percent is divided equally and used for validation and testing purposes. The ABC parameter settings are shown in Table 3. The ABC parameters, such as the size of the bees, are selected as 30 based on the solution space

TABLE 5. Performance evaluation of the proposed ABCNN approach.

Max Generation Size	Proposed ABCNN-RP				Proposed ABCNN-LM				Proposed ABCNN-GD			
	Classification Accuracy (%)		Number of Connections		Classification Accuracy (%)		Number of Connections		Classifiation Accuracy (%)		Number of Connections	
	Best	Mean	Best	Mean	Best	Mean	Best	Mean	Best	Mean	Best	Mean
10	90.31	88.25	19	21.65	86.21	87.22	22	24.52	87.95	88.32	20	21.65
20	93.22	92.37	15	17.25	87.33	88.58	19	21.34	88.60	89.65	18	20.15
30	91.12	89.92	18	19.26	88.03	89.83	18	20.21	89.12	90.67	17	19.03

TABLE 6. Confusion matrix of the proposed ABCNN approach for ten runs.

Method	Actual	Cases	Predicted	
			COVID	Non COVID
ABCNN-RP	COVID	800	740 (TP)	30 (FN)
	Non COVID	380	60 (FP)	350 (TN)
ABCNN-LM	COVID	800	730 (TP)	50 (FN)
	Non COVID	380	70 (FP)	330 (TN)
ABCNN-GD	COVID	800	735 (TP)	45 (FN)
	Non COVID	380	65 (FP)	335 (TN)

considered. The number of employee bees is set equal to the number of onlooker bees following the standard ABC algorithm. The maximum number of iterations is set at 30 considering the computational time. The number of runs is set as 10, where for each iteration size, ten independent runs were executed and the mean accuracy and complexity were calculated.

B. SEGMENTATION PERFORMANCE OF PROPOSED ABCNN

Accuracy based on segmentation results indicates the eventual success or failure of the segmentation process. To evaluate the performance of the segmentation of the proposed ABCNN approach, DICE and Jaccard are used. DICE represents the degree of overlap between two binary images [71] and Jaccard indicates the degree of similarity [72]. These are defined using Equations 10 and 11 in which X and Y indicate the manually segmented infected regions and output image of the optimised region growing segmentation method respectively.

$$DICE(X, Y) = \frac{2|X \cap Y|}{|X| + |Y|} \tag{10}$$

$$Jaccard = |X \cap Y|/|X \cup Y| \tag{11}$$

The segmentation method of the proposed ABCNN approach is applied to the images shown in Figure 7. Examples of segmented portions were shown in Figure 7. The first column shows pre-segmented portions, the middle portion shows ABCNN-based automatic segmentation, which is (Auto-segmented) portions which are segmented by the proposed ABCNN, and the right shows manually segmented portions. Their segmentation results are shown in Table 4.

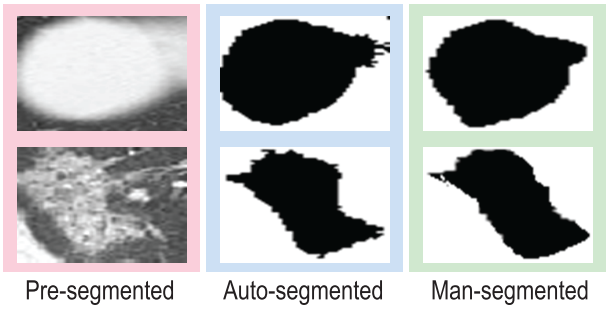

FIGURE 7. Examples of segmented portions. Left shows pre-segmented portions, middle shows ABCNN-based automatic segmented (Auto-segmented) portions, and right shows manually segmented (Man-segmented) portions.

TABLE 7. Performance of ABCNN based on different metrics.

Metrics	Proposed ABCNN -RP	Proposed ABCNN -LM	Proposed ABCNN -GD
Sensitivity (%)	96.10	93.58	94.23
Specificity (%)	85.36	82.50	83.75
Accuracy (%)	92.37	89.83	90.67
Precision (%)	92.5	91.25	91.87
Negative predictive value (%)	92.10	86.84	88.15
F measure	0.9426	0.9240	0.9303

TABLE 8. Performance of ABCNN-RP based on feature selection.

MGS	FS	AHNC	ANSF	ANC	AC
10	WFS	14.4	17.8	21.65	88.25
	WOFS	43.2	20	36.0	80.8
20	WFS	12.1	9.4	17.25	92.37
	WOFS	43.2	20	31.2	81.35
30	WFS	13.6	12.6	19.26	89.92
	WOFS	43.2	20	33.6	80.50

Legend: MGS – Maximum Generalization Size, FS – Feature Selection, AHNC – Average Hidden Node Count, ANSF – Average Number of Selected Features, ANC – Average Number of Connections, AC – Average Accuracy; WFS – With Feature Selection, WOFS – Without Feature Selection.

C. CLASSIFICATION PERFORMANCE OF PROPOSED ABCNN CONCERNING ACCURACY, COMPLEXITY, AND COMPUTATIONAL TIME

The proposed ABCNN approach is investigated for generation sizes of 10, 20, and 30. The number of connections and classification accuracy were calculated for ten independent runs. The backpropagation approaches such as resilient

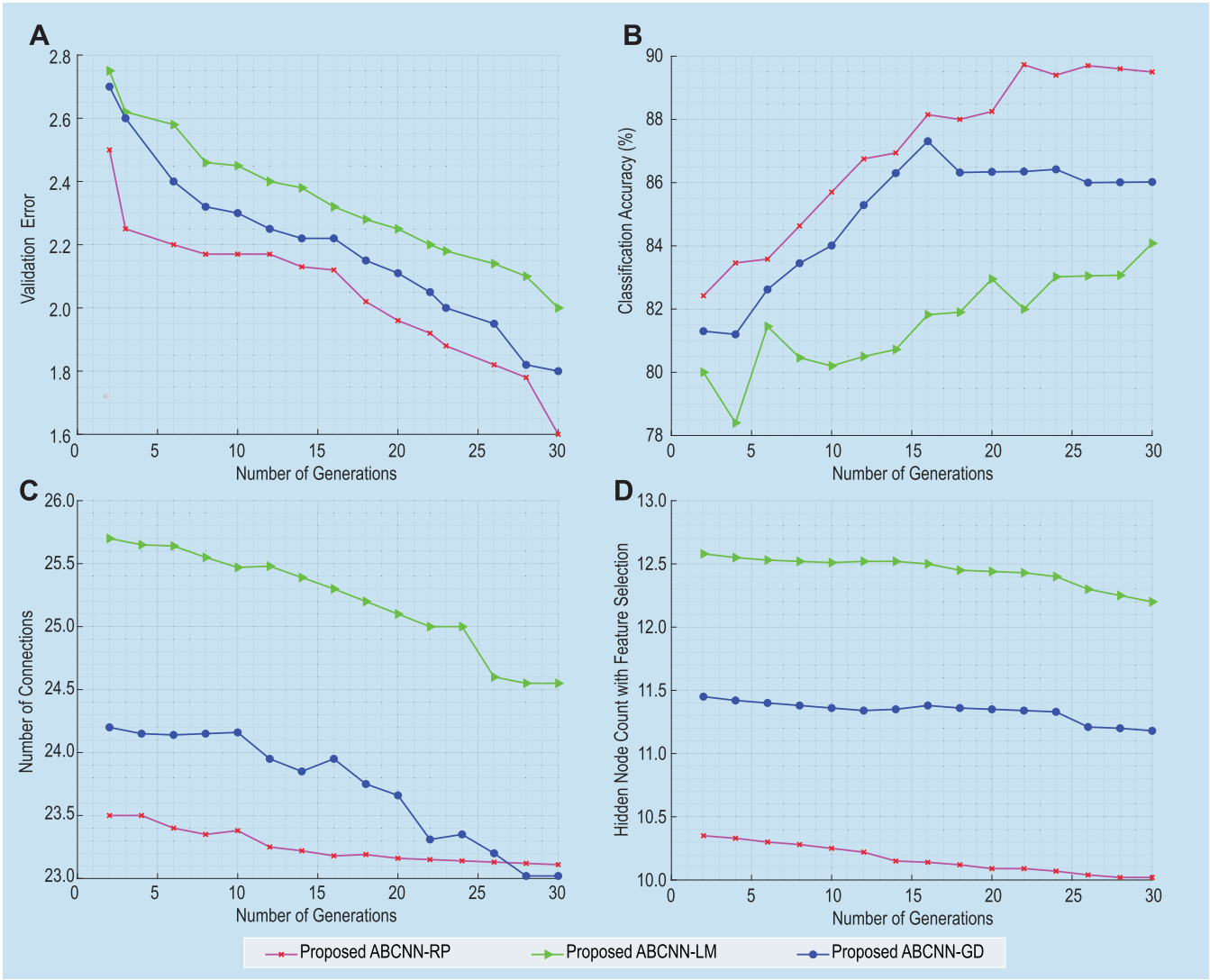

FIGURE 8. Performance of the proposed method. (A) Convergence of Validation error for ABCNN. (B) Performance of ABCNN in terms of classification accuracy. (C) Evolution of the number of connections of ABCNN for different generations. (D) Evolution of hidden node count with feature selection for ABCNN over different generations.

TABLE 9. Confusion matrix of ABCNN-RP for the best network with selected features.

FS	AC		PC		SFS
			Ben	Mal	
WFS	COVID	80	76	4	Entropy, Skewness, Cluster Prominence, Contrast Dissimilarity, Run Length Non-Uniformity, Homogeneity, Gray Level Non-Uniformity
	Non-COVID	38	4	34	
WOFS	COVID	80	68	5	The total dataset from Table 1
	Non-COVID	34	6	28	

Legend: FS – Feature Selection, AC – Actual Cases, PC – Predicted Cases, SFS – Selected Feature Set, WFS – With Feature Selection, WOFS – Without Feature Selection, Ben – Benign, Mal – Malignant.

TABLE 10. Performance of ABCNN-RP based on computational time.

Max.imum Generation Size	Average CPU Time(s) for Proposed Algorithm		
	ABCNN-RP	ABCNN-LM	ABCNN-GD
10	240.2	156.5	455.3
20	505.9	420.6	589.6
30	776.1	654.8	900.6

backpropagation (RP), Levenberg-Marquardt (RM), and momentum-based Gradient Decent (GD) give significant changes in the accuracy and complexity of an ANN model when investigated using the same dataset. Hence, the proposed ABCNN approach is evaluated using RP, LM, and GD, respectively, as given in Table 5. The main aim of

TABLE 11. Performance of ABCNN-RP based on accuracy.

Author, Year	Method	Accuracy
A. M. Hasan, 2020 [57]	DLM	86.7
T. Ozturk, 2020 [60]	DLM	87.02
Wang S, 2020 [61]	DLM	79.3
Butt, 2020 [58]	CNN	86.7
F. Shi, 2020 [73]	RF	87.9
Z. Tang, 2020 [74]	RF	87.5
S. Ying, 2020 [65]	ResNet-50	86.0
M. Fang, 2020 [75]	SVM	82.6
S. Wang, 2020 [76]	DLM	88
W. Shi, 2020 [77]	DLM	89
H. Bai, 2020 [78]	EfficientNet B4 deep neural network	85.00
M. Polsinelli, 2020 [79]	SqueezeNet	83.00
M. Momeny, 2021 [80]	DL & AlexNet	77.60
N. Shadin , 2021 [81]	DL & InceptionV3	85.94
S. Singh, 2021 [82]	DL & LeNet-5/ResNet-50	87.00
Proposed ABCNN	Artificial Bee Colony-Neural Network	84.80

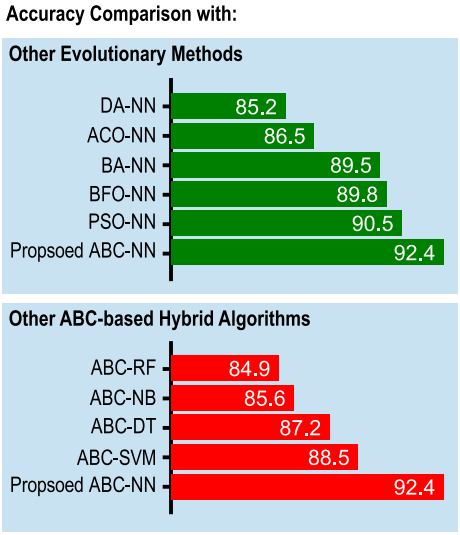

FIGURE 9. Performance comparison in terms of accuracy with other evolutionary methods (top) and other ABC-based hybrid algorithms.

the ABCNN approach is to build an ANN network with an optimal input feature set, initial weights, and hidden node size with less network error, complexity, and computational time. The convergence of validation errors for the ABCNN approach is shown in Figure 8A. The figure shows that ABCNN-RP has produced fewer errors during validation than ABCNN-LM and ABCNN-GD.

ABCNN-RP achieved high classification accuracy (mean) of 92.37% for ten runs at a generation size of 20. Followed by ABCNN-RP, ABCNN-GD achieved a high accuracy of 89.83% at generation 30. Next to ABCNN-GD, ABCNN-LM achieved 90.67% at generation 30. The accuracy attained by ABCNN-RP is 2.83% more than ABCNN-GD and 1.87% more than ABCNN-LM. The average number of connections (average) for ABCNN-RP is 17.25 in the 20th generation size. Followed by ABCNN-RP, ABCNN-GD produced 19.03 mean connections at 30th generation size. Next to ABCNN-GD, ABCNN-LM produced 20.21 mean connections at 30th generation size. ABCNN-RP has generated a less complex ANN compared to the other two variants. ABCNN-RP achieved a complexity of 9.35% less than ABCNN-GD and 14.65% less than ABCNN-LM. Figure 8B depicts the classification accuracy over various runs for different generation sizes for the proposed ABCNN approach.

Figure 8B provides the number of connections used by the ABCNN approach at different generation sizes. According to Figure 8C, ABCNN-RP has utilised fewer connections, leading to a low-complexity network followed by ABCNN-GD and ABCNN-LM. The least number of connections is by ABCNN-RP, which has 15 connections that are 11.76% less than ABCNN-GD and 16.67% less than ABCNN-LM. Figure 8D shows hidden nodes used by the ABCNN approach over different generation sizes.

Table 6 shows the classification performance of the proposed ABCNN approach in using the confusion matrix in terms of True Positive (TP), True Negative (TN), False Positive (FP), and False Negative (FN). A total of 800 COVID cases and 300 non-COVID cases were investigated for ten independent runs.

ABCNN-RP has high sensitivity and specificity, followed by ABCNN-GD and ABCNN-LM, according to Table 7. In Table 8, the performance of ABCNN-RP in terms of the feature selection process is noted since it achieved higher classification accuracy with a low-complexity network. The ABCNN optimised ANN with Feature Selection (FS) has enhanced classification accuracy with low complexity when compared to without FS. Table 9 shows the confusion matrix of ABCNN with RP with the optimally selected feature subsets.

The proposed ABCNN optimised ANN performance concerning computational time is shown in Table 10. The ABCNN-LM requires less computational time than GD and LM. Figure 9 (top) shows the comparison of our ABCNN approach that is based on Artificial Bee Colony optimisation (ABC) with the other swarm intelligent approaches. Because of their extensive global and local search capabilities, we compared the Bat Algorithm (BA), Bacterial Foraging Optimization (BFO), Ant Colony Optimization (ACO),

Dragonfly Algorithm (DA), and Particle Swarm Optimization (PSO). The algorithms considered for comparison are executed using ANN merged with RP using the images collected from [67] similar to our proposed approach. Each algorithm is evaluated for independent 10 runs for 10, 20, and 30 generations, and the highest accuracy achieved is taken and compared with the proposed ABCNN approach. ABCNN achieves high accuracy that is 3.24%, 2.9%, 6.82%, 8.45%, 2.1% more than BA, BFO, ACO, DA, and PSO, respectively.

Figure9 (bottom) shows a comparison of the ABCNN approach on the same dataset with other existing classifiers. The proposed ABCNN has been implemented on various classifiers with the optimal threshold selection for the segmentation process using region growing and also for the feature selection process. We eliminated the process of optimal parameter selection while we executed the classifiers such as SVM, Navie Bayes (NB), Random Forest (RF), and Decision Tree (DT). The proposed ABCNN approach has an accuracy increase of 4.41%, 7.94%, 8.83%, and 5.96% when compared to SVM, NB, RF, and DT, respectively.

Table 11 shows a comparison of the recent COVID-19 diagnosis schemes tested under various datasets involving lung CT and X-ray images with proposed ABCNN. From Table 11, it is evident that the proposed ABCNN has outperformed the COVID-19 diagnosis schemes taken for comparison.

V. CONCLUSION

This paper introduces a computer-aided diagnosis approach based on ABC optimisation called ABCNN. This approach is applied to the lung CT images for segmentation and classification of the abnormal portions. The main strength of the approach lies in its simplicity through a wrapper-based approach and also in deriving optimal parameters for an accurate segmentation and classification process. The computational complexity may be a little high when compared to non-optimized models. The proposed method follows a concurrent feature selection and parameter tuning process. The performance of ABCNN is investigated with various backpropagation algorithms such as RP, LM, and GD using a publicly available lung CT dataset that contains COVID and non-COVID cases. It is concluded that the ABCNN-RP achieved higher accuracy and low complexity than the ANN network. The proposed ABCNN showed promising results when compared with existing work. A comparison of ABCNN with existing swarm intelligent approaches proved better results. In the future, the proposed framework can be applied to the segmentation and classification of high-dimensional COVID-19 datasets by including deep learning models in cloud-based e-Healthcare application servers supporting IoMT.

Conflict of Interest Statement: The authors declare that the research was conducted in the absence of any commercial or financial relationships that could be construed as a potential conflict of interest.

Authors and Contributors: This work was carried out in close collaboration between all co-authors. first defined the research theme and contributed an early design of the system. further implemented and refined the system development. wrote the paper. All authors have contributed to, seen and approved the final manuscript.

Ethical Approval: All procedures performed in studies involving human participants were in accordance with the ethical standards of the institutional and/or national research committee and with the 1964 Helsinki declaration and its later amendments or comparable ethical standards.

Informed Consent: Informed consent was obtained from all individual participants included in the study.

ACKNOWLEDGMENT

The authors are thankful to Qatar National Library (QNL), Qatar, for support to conduct study in this paper.

REFERENCES

[1] WHO. (2020). *Coronavirus Disease (COVID-19) Situation Reports*. Accessed: Jul. 17, 2020. [Online]. Available: https://www.who.int/emergencies/diseases/novel-coronavirus-2019/situation-reports

[2] X. Xie, Z. Zhong, W. Zhao, C. Zheng, F. Wang, and J. Liu, "Chest CT for typical 2019-nCoV pneumonia: Relationship to negative RT-PCR testing," *Radiology*, vol. 296, no. 2, Feb. 2020, Art. no. 200343.

[3] The Novel Coronavirus Pneumonia Emergency Response Epidemiology Team, "The epidemiological characteristics of an outbreak of 2019 novel coronavirus diseases (COVID-19) in China," *Zhonghua Liu Xing Bing Xue Za Zhi Zhonghua Liuxingbingxue Zazhi*, vol. 41, no. 2, p. 145, 2020.

[4] Z. Xie, "Pay attention to SARS-CoV-2 infection in children," *Pediatric Invest.*, vol. 4, no. 1, pp. 1–4, Mar. 2020.

[5] N. Chen, M. Zhou, X. Dong, J. Qu, F. Gong, Y. Han, Y. Qiu, J. Wang, Y. Liu, Y. Wei, J. Xia, T. Yu, X. Zhang, and L. Zhang, "Epidemiological and clinical characteristics of 99 cases of 2019 novel coronavirus pneumonia in Wuhan, China: A descriptive study," *Lancet*, vol. 395, no. 10223, pp. 507–513, Feb. 2020.

[6] X.-W. Xu, X.-X. Wu, X.-G. Jiang, K.-J. Xu, L.-J. Ying, C.-L. Ma, S.-B. Li, H.-Y. Wang, S. Zhang, H.-N. Gao, J.-F. Sheng, H.-L. Cai, Y.-Q. Qiu, and L.-J. Li, "Clinical findings in a group of patients infected with the 2019 novel coronavirus (SARS-Cov-2) outside of Wuhan, China: Retrospective case series," *BMJ*, vol. 368, Feb. 2020, Art. no. m606.

[7] M. Mahmud, M. S. Kaiser, A. Hussain, and S. Vassanelli, "Applications of deep learning and reinforcement learning to biological data," *IEEE Trans. Neural Netw. Learn. Syst.*, vol. 29, no. 6, pp. 2063–2079, Jun. 2018.

[8] M. Mahmud, M. S. Kaiser, T. M. McGinnity, and A. Hussain, "Deep learning in mining biological data," *Cogn. Comput.*, vol. 13, no. 1, pp. 1–33, Jan. 2021.

[9] M. Mahmud and M. S. Kaiser, "Machine learning in fighting pandemics: A COVID-19 case study," in *COVID-19: Prediction, Decision-Making, and its Impacts* (Lecture Notes on Data Engineering and Communications Technologies), vol. 60. Springer, 2021, pp. 77–81.

[10] M. S. Kaiser, S. A. Mamun, M. Mahmud, and M. H. Tania, "Healthcare robots to combat COVID-19," in *COVID-19: Prediction, Decision-Making, and its Impacts* (Lecture Notes on Data Engineering and Communications Technologies), vol. 60. Springer, 2021, pp. 83–97.

[11] S. Tahura, S. M. H. Samiul, K. M. Shamim, and M. Mahmud, "Anomaly detection in electroencephalography signal using deep learning model," in *Proc. Int. Conf. Trends Comput. Cogn. Eng.*, in Advances in Intelligent Systems and Computing, vol. 1309, 2021, pp. 205–217.

[12] M. S. Kaiser, N. Zenia, F. Tabassum, S. A. Mamun, M. A. Rahman, M. S. Islam, and M. Mahmud, "6G access network for intelligent Internet of Healthcare Things: Opportunity, challenges, and research directions," in *Proc. Int. Conf. Trends Comput. Cogn. Eng.*, in Advances in Intelligent Systems and Computing, vol. 1309, 2021, pp. 317–328.

[13] K. M. Shamim, M. Mahmud, M. B. T. Noor, N. Z. Zenia, S. A. Mamun, K. M. A. Mahmud, S. Azad, V. N. M. Aradhya, P. Stephan, T. Stephan, R. Kannan, M. Hanif, T. Sharmeen, T. Chen, and A. Hussain, "*i*Worksafe: Towards healthy workplaces during COVID-19 with an intelligent pHealth app for industrial settings," *IEEE Access*, vol. 9, pp. 13814–13828, 2021.

[14] M. J. A. Nahian, T. Ghosh, M. H. A. Banna, M. A. Aseeri, M. N. Uddin, M. R. Ahmed, M. Mahmud, and M. S. Kaiser, "Towards an accelerometer-based elderly fall detection system using cross-disciplinary time series features," *IEEE Access*, vol. 9, pp. 39413–39431, 2021.

[15] A. K. Singh, A. Kumar, M. Mahmud, M. S. Kaiser, and A. Kishore, "COVID-19 infection detection from chest X-ray images using hybrid social group optimization and support vector classifier," *Cogn. Comput.*, pp. 1–13, Mar. 2021.

[16] M. J. A. Nahian, M. H. Raju, Z. Tasnim, M. Mahmud, M. A. R. Ahad, and M. S. Kaiser, "Contactless fall detection for the elderly," in *Contactless Human Activity Analysis* (Intelligent Systems Reference Library), vol. 200. Springer, 2021, pp. 203–235.

[17] S. Kumar, R. Viral, V. Deep, P. Sharma, M. Kumar, M. Mahmud, and T. Stephan, "Forecasting major impacts of COVID-19 pandemic on country-driven sectors: Challenges, lessons, and future roadmap," *Pers. Ubiquitous Comput.*, pp. 1–24, Mar. 2021, doi: 10.1007/s00779-021-01530-7.

[18] N. Islam, F. Farhin, I. Sultana, M. S. Kaiser, M. S. Rahman, M. Mahmud, A. S. M. S. Hosen, and G. H. Cho, "Towards machine learning based intrusion detection in IoT networks," *Comput., Mater. Continua*, vol. 69, no. 2, pp. 1801–1821, 2021.

[19] S. Zaman, K. Alhazmi, M. A. Aseeri, M. R. Ahmed, R. T. Khan, M. S. Kaiser, and M. Mahmud, "Security threats and artificial intelligence based countermeasures for Internet of Things networks: A comprehensive survey," *IEEE Access*, vol. 9, pp. 94668–94690, 2021.

[20] R. Singh, M. Mahmud, and L. Yovera, "Classification of first trimester ultrasound images using deep convolutional neural network," in *Proc. Int. Conf. Appl. Intell. Inform.*, in Communications in Computer and Information Science, vol. 1435. 2021, pp. 92–105.

[21] P. Mukherjee, I. Bhattacharyya, M. Mullick, R. Kumar, N. D. Roy, and M. Mahmud, "*i*ConDet: An intelligent portable healthcare app for the detection of conjunctivitis," in *Proc. Int. Conf. Appl. Intell. Inform.*, in Communications in Computer and Information Science, vol. 1435. 2021, pp. 29–42.

[22] O. Orojo, J. Tepper, T. M. McGinnity, and M. Mahmud, "Sluggish state-based neural networks provide state-of-the-art forecasts of COVID-19 cases," in *Proc. Int. Conf. Appl. Intell. Inform.*, in Communications in Computer and Information Science, vol. 1435. 2021, pp. 384–400.

[23] S. A. Mamun, M. E. Daud, M. Mahmud, M. S. Kaiser, and A. L. D. Rossi, "ALO: AI for least observed people," in *Proc. Int. Conf. Appl. Intell. Inform.*, in Communications in Computer and Information Science, vol. 1435. 2021, pp. 306–317.

[24] H. Hussain, C.-M. Ting, M. A. Jalil, K. Ray, S. Z. H. Rizvi, J. Kavikumar, F. M. Noman, A. L. A. Zubaidi, Y. F. Low, S. Hussain, M. Mahmud, M. S. Kaiser, and J. Ali, "Identifying individuals using EEG-based brain connectivity patterns," in *Proc. Int. Conf. Brain Inform.*, in Lecture Notes in Computer Science: Including Subseries Lecture Notes in Artificial Intelligence and Lecture Notes in Bioinformatics, vol. 12960, 2021, pp. 124–135.

[25] H. Mukherjee, P. Sreerama, A. Dhar, S. M. Obaidullah, K. Roy, M. Mahmud, and K. C. Santosh, "Automatic lung health screening using respiratory sounds," *J. Med. Syst.*, vol. 45, no. 2, pp. 1–9, Feb. 2021.

[26] Z. S. Shamma, I. J. Rumman, A. M. R. Saikot, S. M. S. Reza, M. M. Islam, M. Mahmud, and M. S. Kaiser, "Kidney care: Artificial intelligence-based mobile application for diagnosing kidney disease," in *Proc. Int. Conf. Data Sci. Appl.*, in Lecture Notes in Networks and Systems, vol. 148, 2021, pp. 99–110.

[27] A. Nawar, N. T. Toma, S. A. Mamun, M. S. Kaiser, M. Mahmud, and M. A. Rahman, "Cross-content recommendation between movie and book using machine learning," in *Proc. IEEE 15th Int. Conf. Appl. Inf. Commun. Technol. (AICT)*, Oct. 2021, pp. 1–6.

[28] M. Biswas, M. H. Tania, M. S. Kaiser, R. Kabir, M. Mahmud, and A. A. Kemal, "ACCU3RATE: A mobile health application rating scale based on user reviews," *PLoS ONE*, vol. 16, no. 12, Dec. 2021, Art. no. e0258050.

[29] Y. Miah, C. N. E. Prima, S. J. Seema, M. Mahmud, and K. M. Shamim, "Performance comparison of machine learning techniques in identifying dementia from open access clinical datasets," in *Advances on Smart and Soft Computing* (Advances in Intelligent Systems and Computing), vol. 1188. 2021, pp. 79–89.

[30] S. I. Tonni, T. A. Aka, M. M. Antik, K. A. Taher, M. Mahmud, and M. S. Kaiser, "Artificial intelligence based driver vigilance system for accident prevention," in *Proc. Int. Conf. Inf. Commun. Technol. Sustain. Develop. (ICICT4SD)*, Feb. 2021, pp. 412–416.

[31] R. V. Tali, S. Borra, and M. Mahmud, "Detection and classification of leukocytes in blood smear images: State of the art and challenges," *Int. J. Ambient Comput. Intell.*, vol. 12, no. 2, pp. 111–139, 2021.

[32] S. W. Yahaya, A. Lotfi, and M. Mahmud, "Towards a data-driven adaptive anomaly detection system for human activity," *Pattern Recognit. Lett.*, vol. 145, pp. 200–207, May 2021.

[33] M. S. Satu, K. C. Howlader, M. Mahmud, M. S. Kaiser, S. M. S. Islam, J. M. W. Quinn, S. A. Alyami, and M. A. Moni, "Short-term prediction of COVID-19 cases using machine learning models," *Appl. Sci.*, vol. 11, no. 9, p. 4266, May 2021.

[34] M. S. Satu, M. I. Khan, M. Mahmud, S. Uddin, M. A. Summers, J. M. W. Quinn, and M. A. Moni, "TClustVID: A novel machine learning classification model to investigate topics and sentiment in COVID-19 tweets," *Knowl.-Based Syst.*, vol. 226, Aug. 2021, Art. no. 107126.

[35] A. K. Singh, G. Sahonero-Alvarez, M. Mahmud, and L. Bianchi, "Towards bridging the gap between computational intelligence and neuroscience in brain-computer interfaces with a common description of systems and data," *Frontiers Neuroinform.*, vol. 15, p. 15, Aug. 2021.

[36] N. B. Prakash, M. Murugappan, G. R. Hemalakshmi, M. Jayalakshmi, and M. Mahmud, "Deep transfer learning for COVID-19 detection and infection localization with superpixel based segmentation," *Sustain. Cities Soc.*, vol. 75, Dec. 2021, Art. no. 103252.

[37] A. Paul, A. Basu, M. Mahmud, M. S. Kaiser, and R. Sarkar, "Inverted bell-curve-based ensemble of deep learning models for detection of COVID-19 from chest X-rays," *Neural Comput. Appl.*, pp. 1–15, Jan. 2022.

[38] I. Kumar, A. Kumar, V. D. A. Kumar, R. Kannan, V. Vimal, K. U. Singh, and M. Mahmud, "Dense tissue pattern characterization using deep neural network," *Cogn. Comput.*, vol. 14, no. 5, pp. 1728–1751, Sep. 2022.

[39] A. Alarjani, M. T. Nasseef, S. M. Kamal, B. V. S. Rao, M. Mahmud, and M. S. Uddin, "Application of mathematical modeling in prediction of COVID-19 transmission dynamics," *Arabian J. Sci. Eng.*, vol. 47, no. 8, pp. 10163–10186, Aug. 2022.

[40] M. Fabietti, M. Mahmud, and A. Lotfi, "Channel-independent recreation of artefactual signals in chronically recorded local field potentials using machine learning," *Brain Informat.*, vol. 9, no. 1, pp. 1–17, Dec. 2022.

[41] S. T. Selvi, S. Arumugam, and L. Ganesan, "BIONET: An artificial neural network model for diagnosis of diseases," *Pattern Recognit. Lett.*, vol. 21, no. 8, pp. 721–740, Jul. 2000.

[42] H. Gadi, G. L. Devi, and N. Ramesh, "Diagnosis of chest diseases using artificial neural networks," in *Internet of Things and Personalized Healthcare Systems*. 2018, pp. 113–119.

[43] M.-Y. Ng, E. Y. P. Lee, J. Yang, F. Yang, X. Li, H. Wang, M. M.-S. Lui, C. S.-Y. Lo, B. Leung, P.-L. Khong, C. K.-M. Hui, K.-Y. Yuen, and M. D. Kuo, "Imaging profile of the COVID-19 infection: Radiologic findings and literature review," *Radiol., Cardiothoracic Imag.*, vol. 2, no. 1, Feb. 2020, Art. no. e200034.

[44] O. Er, N. Yumusak, and F. Temurtas, "Chest diseases diagnosis using artificial neural networks," *Expert Syst. Appl.*, vol. 37, no. 12, pp. 7648–7655, Dec. 2010.

[45] A. R. Patel and M. M. Joshi, "Heart diseases diagnosis using neural network," in *Proc. 4th Int. Conf. Comput., Commun. Netw. Technol. (ICCCNT)*, Jul. 2013, pp. 1–5.

[46] L. Sun, Z. Mo, F. Yan, L. Xia, F. Shan, Z. Ding, B. Song, W. Gao, W. Shao, F. Shi, H. Yuan, H. Jiang, D. Wu, Y. Wei, Y. Gao, H. Sui, D. Zhang, and D. Shen, "Adaptive feature selection guided deep forest for COVID-19 classification with chest CT," *IEEE J. Biomed. Health Informat.*, vol. 24, no. 10, pp. 2798–2805, Oct. 2020.

[47] E. D. Carvalho, E. D. Carvalho, A. O. de Carvalho Filho, F. H. D. de Araùjo, and R. D. A. L. Rabelo, "Diagnosis of COVID-19 in CT image using CNN and XGBoost," in *Proc. ISCC*, Jul. 2020, pp. 1–6.

[48] G. Wang, X. Liu, C. Li, Z. Xu, J. Ruan, H. Zhu, T. Meng, K. Li, N. Huang, and S. Zhang, "A noise-robust framework for automatic segmentation of COVID-19 pneumonia lesions from CT images," *IEEE Trans. Med. Imag.*, vol. 39, no. 8, pp. 2653–2663, Aug. 2020.

[49] X. Wang, X. Deng, Q. Fu, Q. Zhou, J. Feng, H. Ma, W. Liu, and C. Zheng, "A weakly-supervised framework for COVID-19 classification and lesion localization from chest CT," *IEEE Trans. Med. Imag.*, vol. 39, no. 8, pp. 2615–2625, Aug. 2020.

[50] E.-S.-M. El-Kenawy, A. Ibrahim, S. Mirjalili, M. M. Eid, and S. E. Hussein, "Novel feature selection and voting classifier algorithms for COVID-19 classification in CT images," *IEEE Access*, vol. 8, pp. 179317–179335, 2020.
[51] S. Sakib, T. Tazrin, M. M. Fouda, Z. M. Fadlullah, and M. Guizani, "DL-CRC: Deep learning-based chest radiograph classification for COVID-19 detection: A novel approach," *IEEE Access*, vol. 8, pp. 171575–171589, 2020.
[52] S. Rajaraman, J. Siegelman, P. O. Alderson, L. S. Folio, L. R. Folio, and S. K. Antani, "Iteratively pruned deep learning ensembles for COVID-19 detection in chest X-rays," *IEEE Access*, vol. 8, pp. 115041–115050, 2020.
[53] A. K. Mishra, S. K. Das, P. Roy, and S. Bandyopadhyay, "Identifying COVID19 from chest CT images: A deep convolutional neural networks based approach," *J. Healthcare Eng.*, vol. 2020, pp. 1–7, Aug. 2020.
[54] D. Singh, V. Kumar, Vaishali, and M. Kaur, "Classification of COVID-19 patients from chest CT images using multi-objective differential evolution–based convolutional neural networks," *Eur. J. Clin. Microbiol. Infectious Diseases*, vol. 39, no. 7, pp. 1379–1389, Jul. 2020.
[55] C. Goel, A. Kumar, S. K. Dubey, and V. Srivastava, "Efficient deep network architecture for COVID-19 detection using computed tomography images," *medRxiv*, 2020.
[56] R. Jain, M. Gupta, S. Taneja, and D. J. Hemanth, "Deep learning based detection and analysis of COVID-19 on chest X-ray images," *Int. J. Speech Technol.*, vol. 51, no. 3, pp. 1690–1700, Mar. 2021.
[57] A. M. Hasan, M. M. Al-Jawad, H. A. Jalab, H. Shaiba, R. W. Ibrahim, and A. R. Al-Shamasneh, "Classification of COVID-19 coronavirus, pneumonia and healthy lungs in CT scans using *Q*-deformed entropy and deep learning features," *Entropy*, vol. 22, no. 5, p. 517, May 2020.
[58] X. Xu, X. Jiang, C. Ma, P. Du, X. Li, S. Lv, and L. Li, "A deep learning system to screen novel coronavirus disease 2019 pneumonia," *Engineering*, vol. 6, no. 10, pp. 1122–1129, 2020.
[59] L. Li, L. Qin, Z. Xu, Y. Yin, X. Wang, B. Kong, J. Bai, Y. Lu, Z. Fang, Q. Song, K. Cao, D. Liu, G. Wang, Q. Xu, X. Fang, S. Zhang, J. Xia, and J. Xia, "Artificial intelligence distinguishes COVID-19 from community acquired pneumonia on chest CT," *Radiology*, vol. 296, no. 2, Mar. 2020, Art. no. 200905.
[60] T. Ozturk, M. Talo, E. A. Yildirim, U. B. Baloglu, O. Yildirim, and U. R. Acharya, "Automated detection of COVID-19 cases using deep neural networks with X-ray images," *Comput. Biol. Med.*, vol. 121, Jun. 2020, Art. no. 103792.
[61] S. Wang, B. Kang, J. Ma, X. Zeng, M. Xiao, J. Guo, M. Cai, J. Yang, Y. Li, X. Meng, and B. Xu, "A deep learning algorithm using CT images to screen for corona virus disease (COVID-19)," *medRxiv*, 2020.
[62] C. Zheng, X. Deng, Q. Fu, Q. Zhou, J. Feng, H. Ma, W. Liu, and X. Wang, "Deep learning-based detection for COVID-19 from chest CT using weak label," *medRxiv*, 2020.
[63] M. Toğaçar, B. Ergen, and Z. Cömert, "COVID-19 detection using deep learning models to exploit social mimic optimization and structured chest X-ray images using fuzzy color and stacking approaches," *Comput. Biol. Med.*, vol. 121, Jun. 2020, Art. no. 103805.
[64] M. Barstugan, U. Ozkaya, and S. Ozturk, "Coronavirus (COVID-19) classification using CT images by machine learning methods," 2020, *arXiv:2003.09424*.
[65] S. Ying, S. Zheng, L. Li, X. Zhang, X. Zhang, Z. Huang, J. Chen, H. Zhao, R. Wang, Y. Chong, J. Shen, Y. Zha, and Y. Yang, "Deep learning enables accurate diagnosis of novel coronavirus (COVID-19) with CT images," *medRxiv*, vol. 18, no. 6, 2020.
[66] X. Chen, L. Yao, and Y. Zhang, "Residual attention U-Net for automated multi-class segmentation of COVID-19 chest CT images," 2020, *arXiv:2004.05645*.
[67] X. Yang, X. He, J. Zhao, Y. Zhang, S. Zhang, and P. Xie, "COVID-CT-dataset: A CT scan dataset about COVID-19," 2020, *arXiv:2003.13865*.
[68] A. Telikani, A. H. Gandomi, A. Shahbahrami, and M. Naderi Dehkordi, "Privacy-preserving in association rule mining using an improved discrete binary artificial bee colony," *Expert Syst. Appl.*, vol. 144, Apr. 2020, Art. no. 113097.
[69] S. Punitha, A. Amuthan, and K. S. Joseph, "Enhanced monarchy butterfly optimization technique for effective breast cancer diagnosis," *J. Med. Syst.*, vol. 43, no. 7, p. 206, Jul. 2019.
[70] S.-M. Lai, X. Li, and W. F. Biscof, "On techniques for detecting circumscribed masses in mammograms," *IEEE Trans. Med. Imag.*, vol. 8, no. 4, pp. 377–386, Dec. 1989.
[71] L. R. Dice, "Measures of the amount of ecologic association between species," *Ecology*, vol. 26, no. 3, pp. 297–302, Jul. 1945.
[72] A. H. Cheetham and J. E. Hazel, "Binary (presence-absence) similarity coefficients," *J. Paleontol.*, vol. 43, no. 5, pp. 1130–1136, 1969.
[73] F. Shi, L. Xia, F. Shan, D. Wu, Y. Wei, H. Yuan, H. Jiang, Y. Gao, H. Sui, and D. Shen, "Large-scale screening of COVID-19 from community acquired pneumonia using infection size-aware classification," 2020, *arXiv:2003.09860*.
[74] Z. Tang, W. Zhao, X. Xie, Z. Zhong, F. Shi, J. Liu, and D. Shen, "Severity assessment of coronavirus disease 2019 (COVID-19) using quantitative features from chest CT images," 2020, *arXiv:2003.11988*.
[75] M. Fang, B. He, L. Li, D. Dong, X. Yang, C. Li, L. Meng, L. Zhong, H. Li, H. Li, and J. Tian, "CT radiomics can help screen the coronavirus disease 2019 (COVID-19): A preliminary study," *Sci. China Inf. Sci.*, vol. 63, no. 7, Jul. 2020, Art. no. 172103.
[76] S. Wang, Y. Zha, W. Li, Q. Wu, X. Li, M. Niu, M. Wang, X. Qiu, H. Li, H. Yu, W. Gong, Y. Bai, L. Li, Y. Zhu, L. Wang, and J. Tian, "A fully automatic deep learning system for COVID-19 diagnostic and prognostic analysis," *Eur. Respiratory J.*, vol. 56, no. 2, Aug. 2020, Art. no. 2000775.
[77] W. Shi, X. Peng, T. Liu, Z. Cheng, H. Lu, S. Yang, J. Zhang, F. Li, M. Wang, X. Zhang, Y. Gao, Y. Shi, Z. Zhang, and F. Shan, "Deep learning-based quantitative computed tomography model in predicting the severity of COVID-19: A retrospective study in 196 patients," *SSRN Electron. J.*, 2020.
[78] H. X. Bai, R. Wang, Z. Xiong, B. Hsieh, K. Chang, K. Halsey, T. M. Tran, J. W. Choi, D.-C. Wang, L.-B. Shi, J. Mei, X.-L. Jiang, I. Q.-H. P. Zeng, P.-F. Hu, Y.-H. Li, F.-X. Fu, R. Y. Huang, R. Sebro, and W.-H. Liao, "Artificial intelligence augmentation of radiologist performance in distinguishing COVID-19 from pneumonia of other origin at chest CT," *Radiology*, vol. 299, no. 1, p. E225, Apr. 2021.
[79] M. Polsinelli, L. Cinque, and G. Placidi, "A light CNN for detecting COVID-19 from CT scans of the chest," *Pattern Recognit. Lett.*, vol. 140, pp. 95–100, Dec. 2020.
[80] M. Momeny, A. A. Neshat, M. A. Hussain, S. Kia, M. Marhamati, A. Jahanbakhshi, and G. Hamarneh, "Learning-to-augment strategy using noisy and denoised data: Improving generalizability of deep CNN for the detection of COVID-19 in X-ray images," *Comput. Biol. Med.*, vol. 136, Sep. 2021, Art. no. 104704.
[81] N. S. Shadin, S. Sanjana, and N. J. Lisa, "COVID-19 diagnosis from chest X-ray images using convolutional neural network (CNN) and inceptionV3," in *Proc. Int. Conf. Inf. Technol. (ICIT)*, Jul. 2021, pp. 799–804.
[82] S. Singh, P. Sapra, A. Garg, and D. K. Vishwakarma, "CNN based COVID-aid: COVID 19 detection using chest X-ray," in *Proc. 5th Int. Conf. Comput. Methodol. Commun. (ICCMC)*, Apr. 2021, pp. 1791–1797.
[83] G. Chandrasekaran, S. Periyasamy, and K. P. Rajamanickam, "Minimization of test time in system on chip using artificial intelligence-based test scheduling techniques," *Neural Comput. Appl.*, vol. 32, no. 9, pp. 5303–5312, May 2020.
[84] G. Chandrasekaran, P. R. Karthikeyan, N. S. Kumar, and V. Kumarasamy, "Test scheduling of system-on-chip using dragonfly and ant lion optimization algorithms," *J. Intell. Fuzzy Syst.*, vol. 40, no. 3, pp. 4905–4917, Mar. 2021.
[85] G. Chandrasekaran, S. Periyasamy, and P. R. Karthikeyan, "Test scheduling for system on chip using modified firefly and modified ABC algorithms," *Social Netw. Appl. Sci.*, vol. 1, no. 9, pp. 1–12, Sep. 2019.
[86] G. Chandrasekaran, V. Kumarasamy, and G. Chinraj, "Test scheduling of core based system-on-chip using modified ant colony optimization," *J. Européen des Systèmes Automatisés*, vol. 52, no. 6, pp. 599–605, Dec. 2019.

S. PUNITHA received the B.E. and M.E. degrees in computer science and engineering from Anna University, India, and the Ph.D. degree in computer science and engineering from Pondicherry University, India. She has published her research works in reputed journals, conferences, patents, and book chapters. Her research interests include medical image analysis, evolutionary computation, artificial intelligence, and machine learning techniques.

THOMPSON STEPHAN (Member, IEEE) received the B.E. and M.E. degrees in computer science and engineering from Anna University, India, and the Ph.D. degree in computer science and engineering from Pondicherry University, India. He is currently holding the position of an Assistant Professor at the Department of Computer Science and Engineering, Faculty of Engineering and Technology, M. S. Ramaiah University of Applied Sciences, India. He has authored many technical research papers published in leading journals and conferences by the IEEE, Elsevier, and Springer. His research interests include on the implementation and practical applications of artificial intelligence techniques. He was awarded for his academic excellence in his master's degree with a university rank. He received the Best Researcher Award-2020 from the IEEE Bengaluru Section, India. He is an active reviewer of many internationally reputed journals and a book editor.

RAMANI KANNAN (Senior Member, IEEE) received the bachelor's degree in electronics and communication engineering from Bharathiyar University, India, and the master's and Doctoral degrees in electrical and electronics engineering specializing in power electronics and drives from Anna University, India. He is a Senior Lecturer and a Postgraduate Program Leader at the Department of Electrical and Electronics Engineering, Universiti Teknologi PETRONAS, Malaysia. He has published more than 125 research papers and ten book chapters, extensively in international journals and forums with a good number of citations. He has handled a number of industry/government-funded projects and schemes. He has been the Chair of IEEE PELS, Malaysia Chapter, since 2022. He is served as an editor and a reviewer for many national and international conferences and journals with high repute.

MUFTI MAHMUD (Senior Member, IEEE) is an Associate Professor of cognitive computing at the Department of Computer Science, Nottingham Trent University (NTU). He has been listed among the top 2% cited scientists worldwide in computer science in 2020. His research interests include computational-, health- and social- sciences, and uses of neuroscience, healthcare, applied data science, computational neuroscience, big data analytics, cyber security, machine learning, cloud computing, software engineering, and plans to develop secure computational tools to advance healthcare access in low-resource settings. He is a fellow of the Higher Education Academy, a Senior Member of the Association of Computing Machinery (ACM), and a Professional Member of the British Computer Society (BCS). He was the winner of the 2021 Vice-Chancellor's Outstanding Research Award for Early Career Researchers. He also serves as the Vice-Chair of the Intelligent System Application Technical Committee of the IEEE Computational Intelligence Society (CIS). As per Scopus, he holds the highest number of publications among the academics from universities in Nottinghamshire in the computer science domain from January 2018 to March 2022. Also, by Scopus, he has been ranked as the third top during the same period among computer science academics from universities in the East Midlands region. He is a Section Editor (big data analytics) of the *Cognitive Computation* journal, the Regional Editor (Europe) of the *Brain Informatics* journal, and an Associate Editor (neuroprosthetics) of the *Frontiers in Neuroscience* journal.

M. SHAMIM KAISER (Senior Member, IEEE) received the bachelor's and master's degrees in applied physics electronics and communication engineering from the University of Dhaka, Bangladesh, in 2002 and 2004, respectively, and the Ph.D. degree in telecommunication engineering from the Asian Institute of Technology (AIT) Pathumthani, Thailand, in 2010. He is currently working as a Professor at the Institute of Information Technology, Jahangirnagar University, Savar, Dhaka, Bangladesh. He worked as a Postdoctoral Fellow at the Big Data and Cyber Security Laboratory, Anglia Ruskin University, U.K., from 2017 to 2018. He also worked as a Special Research Student at the Wireless Signal Processing and Networking Laboratory (Adachi Lab), Tohoku University, Japan, in 2008. He has authored more than 150 papers in different peer-reviewed journals and conferences. His current research interests include data analytics, machine learning, wireless networks, signal processing, cognitive radio networks, the big IoT data, healthcare, neuroinformatics, and cyber security. He is a Life Member of Bangladesh Electronic Society, Bangladesh Physical Society, and NOAMI. He is also a Senior Member of IEICE, Japan, and an Active Volunteer of the IEEE Bangladesh Section. He is the founding Chapter Chair of the IEEE Bangladesh Section Computer Society Chapter. He is an Academic Editor of *PLOS One* journal; an Associate Editor of IEEE Access and *Cognitive Computation* journal, the Guest Editor of *Brain Informatics* journal, *IJACI* (IGI Global), *Electronics* (MDPI), *Frontiers in Neuroinformatics*, and *Cognitive Computation* journal.

SAMIR BRAHIM BELHAOUARI, photograph and biography not available at the time of publication.